High Doses of Bone Morphogenetic Protein 2 Induce Structurally Abnormal Bone and Inflammation *In Vivo*

Janette N. Zara, M.D.,[1,2,*] Ronald K. Siu, M.S.,[1,2,*] Xinli Zhang, M.D., Ph.D.,[2] Jia Shen, Ph.D.,[1,2] Richard Ngo,[2] Min Lee, Ph.D.,[3] Weiming Li, M.D.,[2,4] Michael Chiang, B.D.S.,[2] Jonguk Chung, B.S.,[2] Jinny Kwak, D.D.S.,[2] Benjamin M. Wu, D.D.S., Ph.D.,[1] Kang Ting, D.M.D., DMedSci.,[1,2,†] and Chia Soo, M.D.[5,†]

The major Food and Drug Association–approved osteoinductive factors in wide clinical use are bone morphogenetic proteins (BMPs). Although BMPs can promote robust bone formation, they also induce adverse clinical effects, including cyst-like bone formation and significant soft tissue swelling. In this study, we evaluated multiple BMP2 doses in a rat femoral segmental defect model and in a minimally traumatic rat femoral onlay model to determine its dose-dependent effects. Results of our femoral segmental defect model established a low BMP2 concentration range (5 and 10 µg/mL, total dose 0.375 and 0.75 µg in 75 µg total volume) unable to induce defect fusion, a mid-range BMP2 concentration range able to fuse the defect without adverse effects (30 µg/mL, total dose 2.25 µg in 75 µg total volume), and a high BMP2 concentration range (150, 300, and 600 µg/mL, total dose 11.25, 22.5, and 45 µg in 75 µg total volume) able to fuse the defect, but with formation of cyst-like bony shells filled with histologically confirmed adipose tissue. In addition, compared to control, 4 mg/mL BMP2 also induced significant tissue inflammatory infiltrates and exudates in the femoral onlay model that was accompanied by increased numbers of osteoclast-like cells at 3, 7, and 14 days. Overall, we consistently reproduced BMP2 side effects of cyst-like bone and soft tissue swelling using high BMP2 concentration approaching the typical human 1500 µg/mL.

Introduction

BONE MORPHOGENETIC PROTEIN 2 (BMP2) is the leading osteoinductive growth factor used clinically in bone-related regenerative medicine today. The Food and Drug Association has approved the use of INFUSE® Bone Graft (BMP2) to enhance the growth of bone in specific clinical scenarios, including anterior and lumbar interbody spine fusion and open tibial fractures.[1,2] However, in these applications BMP2 is needed at supraphysiologic doses to induce human osteogenesis.[3] The high BMP doses in clinical use may contribute to numerous adverse effects in humans not seen in rodent animal models, including ectopic bone formation with spinal cord impingement,[4] osteoclast activation with transiently elevated bone resorption,[5] cyst-like bone void formation, and life-threatening cervical swelling. Interestingly, in most cases involving cervical swelling, emergent operative re-exploration did not identify any drainable fluid

collections (e.g., hematoma).[6] Instead, diffuse soft-tissue swelling, presumably inflammatory in nature, was noted in the anterior neck structures such as the esophagus and strap muscles.[6,7] Although proven as an effective osteoinducer, these adverse effects, along with the possibility of forming structurally abnormal and potentially mechanically unstable bone tissue, currently limit the overall clinical efficacy of BMPs. The ability to define upper and lower bounds for BMP doses that would both form high-quality bone and avoid swelling, void formation, and other side effects would improve the prospects of BMP as a tissue engineering adjunct and as a clinical product.

From studies in various animal models, BMPs are known to have species-specific osteoinductive dose requirements. The minimum dose of BMPs necessary to induce consistent bone formation is substantially higher in nonhuman primates than in rodents. For example, in rats 0.2–0.4 mg/mL BMP2 is effectively osteoinductive, whereas sheep and pri-

[1]Department of Bioengineering, University of California, Los Angeles, California.
[2]Dental and Craniofacial Research Institute, School of Dentistry, University of California, Los Angeles, California.
[3]Division of Advanced Prosthodontics, Biomaterials, and Hospital Dentistry, University of California, Los Angeles, California.
[4]Department of Orthopaedics, First Clinical Hospital, Harbin Medical University, Harbin, China.
[5]Department of Orthopaedic Surgery, School of Medicine, University of California, Los Angeles, California.
*Co-first authors.
†Co-senior authors.

mates require higher concentrations of 0.43 and 0.75–1.5 mg/mL BMP2, respectively.[8–10] The 1.5 mg/mL concentration used for initial human clinical trials in anterior interbody spine fusion was based on this nonhuman primate data and is currently the approved concentration for human use.[11] The wide species-specific differential in osteoinductive BMP2 dose requirements may account for the lack of BMP2-related side effects in animal models such as rodents, where bone formation is achieved at much lower doses at which these side effects are not observed.

With the increasing reports of BMP2-induced side effects, and the recent Food and Drug Association panel's decision to recommend approval of AMPLIFY™, a higher 2.0 mg/mL concentration BMP2 product for posterolateral spine fusion, there is an even more compelling reason to elucidate the molecular basis for adverse BMP2 effects. As a first step, we determined if clinical BMP2 side effects such as cyst-like bone void formation and tissue inflammation/swelling were consistently reproducible in rodent models in a dose-dependent fashion. To reproduce cyst-like bone void formation, we tested escalating BMP2 doses in a traumatic rat femoral segmental defect model. This is a stringent, well-described bone regeneration model in which the central third of the femur is excised and replaced with bone grafting material.[12] To reproduce BMP2-mediated soft tissue inflammatory swelling, we utilized a minimally traumatic model in which collagen sponges soaked with BMP2 are laid over periosteally intact bone, similar to collagen sponge onlay models used by others.[13] The less traumatic onlay model was specifically chosen to minimize surgery-associated inflammation and facilitate delineation of BMP2-induced inflammation.

Materials and Methods

Implant materials

For femoral segmental defects, apatite-coated poly(lactic-co-glycolic acid) (PLGA) scaffolds were fabricated from 85/15 PLGA by solvent casting and a particulate leaching process (Fig. 1). Briefly, PLGA/chloroform solutions mixed with 200–300-μm-diameter sucrose (polymer/sucrose ratio 5/95, w/w) was cast into a Teflon mold to create a cylindrical construct (4 mm diameter, 6 mm length). After freeze-drying overnight, scaffolds were removed from the Teflon mold and immersed in ddH_2O to dissolve the sucrose. Scaffolds were disinfected by immersion in 70% ethanol for 30 min, and followed by three rinses of ddH_2O.

To ensure efficient BMP2 loading and to enhance overall osteoconductivity of the hydrophobic PLGA scaffold, the scaffold surface was treated with a biomimetic apatite coating process before impregnation with varying doses of recombinant human BMP2 protein (rhBMP2; Medtronic, Minneapolis, MN), as described in our previous studies.[14,15] For apatite coating, simulated body fluid (SBF) solution was prepared by sequentially dissolving $CaCl_2$, $MgCl_2 \cdot 6H_2O$, $NaHCO_3$, and $K_2HPO_4 \cdot 3H_2O$ in ddH_2O. Solution pH was lowered to 6 by adding 1M hydrochloric acid to increase solubility. Na_2SO_4, KCl, and NaCl were added and the final pH was adjusted to 6.5 (SBF 1). Mg^{2+} and HCO_3^- free SBF (SBF 2) was prepared by adding $CaCl_2$ and $K_2HPO_4 \cdot 3H_2O$ in ddH_2O and pH was lowered to 6. KCl and NaCl were added and the final pH was adjusted to 6.8. All solutions
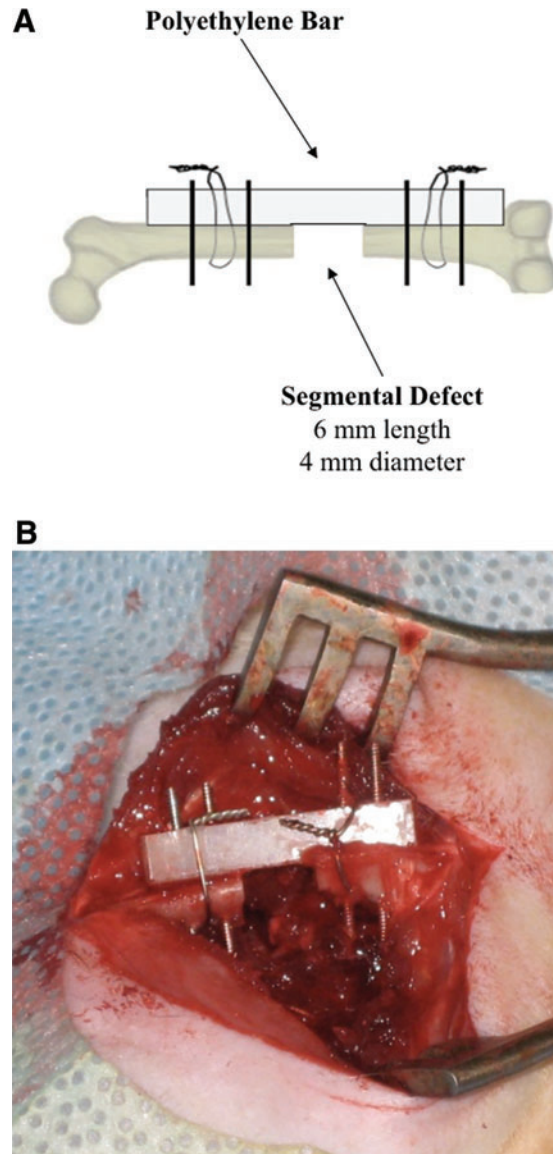
FIG. 1. Femoral segmental defect model. **(A)** Schematic diagram depicting use of two Kirschner wires and a cerclage wire on either side of the defect to affix the polyethylene plate to the femur; **(B)** intraoperative photograph. Color images available online at www.liebertonline.com/tea

were sterile filtered through a 0.22 μm polyethersulfone membrane (Nalgene, Penfield, NY). Immediately before the coating process, the dried PLGA scaffolds were subjected to glow discharge argon plasma etching (Harrick Scientific, Ossining, NY) to improve wetting and coating uniformity. Etched scaffolds were then incubated in SBF 1 for 12 h and changed to Mg^{2+} and HCO_3^- free SBF 2 for another 12 h at 37°C under gentle stirring. Coated scaffolds were washed with ddH_2O to remove excess ions and lyophilized before further studies.

Surgical procedure and study groups

All surgical procedures were approved by the UCLA Chancellor's Animal Research Committee. The two surgical procedures performed were creation of a femoral segmental

defect followed by material implantation into the defect or an onlay graft of a collagen sponge onto the femoral surface. Animals were anesthetized by isoflurane inhalation. After surgery, all animals were housed in separate cages and allowed to eat and drink *ad libitum*. Weight bearing was started immediately postoperatively, with daily monitoring. Buprenorphine was administered for 2 days as an analgesic, and trimethoprim/sulfamethoxazole was administered for 10 days as an antibiotic.

Femoral segmental defect. Twenty-two male Lewis rats between 12 and 14 weeks of age were randomized into seven experimental implant groups: PLGA with (1) phosphate-buffered saline (PBS) only (control), or PLGA with rhBMP2 at (2) 5 μg/mL, (3) 10 μg/mL, (4) 30 μg/mL, (5) 150 μg/mL, (6) 300 μg/mL, and (7) 600 μg/mL. The volume of all scaffolds is 75 μL; thus, the total rhBMP2 dose per defect in each group is (1) 0 μg, (2) 0.375 μg, (3) 0.75 μg, (4) 2.25 μg, (5) 11.25 μg, (6) 22.5 μg, and (7) 45 μg, respectively (Table 1). The rat femoral segmental defect is a well-established model in which the defect does not heal with an osteoconductive material alone, but requires an additional osteoinductive agent such as rhBMP2 to achieve union.[12,16–18] The remaining concentrations were selected based on previously published studies on BMP2 in rodents that include an ineffective range of 7 to 18.7 μg/mL (1.4 μg rhBMP2 in 75–200 μL of carrier),[19] an effective range of 55–146.7 μg/mL (11 μg rhBMP2 in 75–200 μL of carrier),[19,20] as well as higher concentrations to represent those used clinically. The surgical procedure was similar to that reported elsewhere[19] with modifications, and summarized briefly here. Using aseptic technique, a 25–30 mm longitudinal incision was made over the anterolateral aspect of the femur. The vastus lateralis and biceps femoris muscles were separated, exposing the femoral shaft. A polyethylene plate (length, 23 mm; width, 4 mm; height, 4 mm) was placed on the anterolateral surface of the femur. The plate contained four predrilled holes to accommodate 0.9-mm-diameter threaded Kirschner wires. Taking the plate as a template, four threaded Kirschner wires were drilled through the plate and both cortices. Two 26-gauge stainless steel cerclage wires were tightened around the plate

and bone for additional stability. With a small oscillating saw blade (Stryker, Kalamazoo, MI), a 6-mm critical-sized[12] mid-diaphyseal defect was created (Fig. 1). The volume of the defect was ~75 μL. An implant was placed into the defect, and then the overlying muscle and fascia were closed with 4–0 Vicryl absorbable suture to secure the implant in place. 4–0 Vicryl was also used to close the skin in a running subcuticular fashion. Animals were euthanized at 8 weeks postoperation.

Onlay graft. Seventeen male Lewis rats aged 12–14 weeks were randomized into 3 experimental groups according to sacrifice timepoints of 3, 7, or 14 days postoperation (Table 2). For onlay model implants, Helistat absorbable collagen sponges (ACS; thickness 1 mm, porosity 88.2%[21]; Integra, Plainsboro, NJ) were cut into 1×2 cm strips and sterilized before surgery. Sponges were saturated by dropwise application of 0.2 mL of either 4 mg/mL rhBMP2 in PBS (experimental; total dose: 0.8 mg rhBMP2) or PBS only (control), and allowed to soak for 15 min before implantation. For each timepoint, one animal was implanted with control ACS on both limbs to exclude nonspecific inflammation induced by the ACS itself.[22] In the remaining animals, one hind limb was implanted with ACS plus PBS (control); the contralateral side was implanted with ACS plus 4 mg/mL rhBMP2. After anesthesia, the hind limbs were shaved and a transverse incision was made at the level of the midpoint of the femur. The vastus lateralis and biceps femoris were elevated through an anterolateral approach with care to keep the periosteum intact along the surface of the bone. Each ACS was placed over the femoral surface, adjacent to the muscle, fascia, and skin. Each layer was closed with 4–0 Vicryl suture as described above. Animals were sacrificed at 3, 7, and 14 days postoperation depending on experimental group assignment.

Radiographic evaluation

For the femoral segmental defect model, high-resolution lateral radiographs were obtained at 2, 4, 6, and 8 weeks after implantation while the animals were under isoflurane sedation. Three observers, blinded to the treatment variables, scored defect mineralization with a standardized scale adapted from Kirker-Head *et al.*[23] as follows: 0, trace radiodense material in defect; 1, flocculent radiodensity and incomplete bridging of defect; 2, bridging of the defect at 1+ location; 3, bridging of the defect at *cis* and *trans* cortices, parent cortex visible; 4, one cortex obscured by new bone; 5, bridging of the defect by uniform new bone, cut ends of cortex not seen.

Three-dimensional micro-computed tomography evaluation

At 8 weeks postoperation, all femoral segmental defect animals were euthanized. The femurs were dissected, harvested, and fixed in 10% buffered formalin (Fisher Scientific, Fair Lawn, NJ). After fixation for a minimum of 48 h, the samples were scanned in the axial plane using a three-dimensional micro-computed tomography (microCT) scanner (μCT 40, Scanco Medical, Bassersdorf, Switzerland; Skyscan, Kontich, Belgium) at 20 μm resolution. After scanning, the μCT 40 software was used to analyze and measure

TABLE 1. FEMORAL SEGMENTAL DEFECT IMPLANT FORMULATION AND EXPERIMENTAL GROUP DESIGNATIONS

Experimental group (concentration, μg/mL rhBMP2)	Scaffold volume (μL)	Total rhBMP2 dose (μg)	n	% fused	% cyst
PBS only	75	0	2	0	0
5	75	0.375	4	0	0
10	75	0.75	4	0	0
30	75	2.25	3	100	0
150	75	11.25	3	100	0
300	75	22.5	3	100	66
600	75	45	3	100	100

Radiographic evaluation showed 100% fusion of defect at 30 μg/mL BMP2 and higher, and 0% fusion at lower concentrations. 66% and 100% cyst formation was seen in 300 and 600 μg/mL rhBMP2 groups, respectively.

PBS, phosphate-buffered saline; rhBMP2, recombinant human bone morphogenetic protein 2.

Days	Volume of rhBMP2 solution (µL)	rhBMP2 concentration (mg/mL)	Total rhBMP2 incorporated (µg)	Number of control implantations	Number of rhBMP2 implantations	Total animals operated
3	200	4	800	8	4	6
7	200	4	800	9	5	7
14	200	4	800	6	2	4

the bone volume in the defect where the implant was placed. A constant volume of interest, 300 slices thick (~ 6 mm) and centered over the defect site, was selected for analysis of all samples. The bone volume per defect was recorded as the measure of segmental defect bone regeneration.

Histological assessment

After microCT analysis, the femoral segmental defect specimens were decalcified using Cal-Ex solution (Fisher Scientific, Pittsburgh, PA) for 5 to 7 days, washed with running tap water for 3 to 4 h, and then transferred to 75% ethanol solution. The specimens were embedded in paraffin and 5 µm sagittal sections of each specimen were obtained and then stained with hematoxylin and eosin (H&E) and Masson's Trichrome stains. Immunohistochemistry staining for osteocalcin (OCN) was performed to detect active bone formation.

For onlay graft animals, tissue from the biceps femoris, vastus lateralis, and the femur and its overlying periosteum adjacent to and inclusive of the collagen sponge were harvested after sacrifice and fixed in formalin as described above. H&E was performed to delineate cellular infiltrates and immunohistochemistry for calcitonin receptor (CTR) was performed to detect presence of osteoclastic cells.[24]

Statistical analysis

Mann–Whitney and Kruskal–Wallis tests were used to compare radiographic scores, and Student's t-test and analysis of variance were used to compare bone volume measurements between groups. $p < 0.05$ was considered statistically significant.

Results

Radiographic data

X-ray images showed that of the rhBMP2 doses tested, the most robust bone formed when a concentration of 30 µg/mL rhBMP2 (2.25 µg total dose) was added to the defect, achieving 100% fusion (Table 1). In some cases, new bone within the defect was indistinguishable from the native bone proximal and distal to the defect space. When concentrations <30 µg/mL were used (0, 5, or 10 µg/mL rhBMP2), defect union was incomplete as expected, with no evidence of bridging bone between the two ends of the defect. However, when 150 µg/mL rhBMP2 and higher (300 or 600 µg/mL) were used, bone fusion was achieved, but radiolucent voids within the bone in the defect space and heterotopic bone formation outside of the defect space were observed (Faxitron X-ray images not shown; microCT two-dimensional X-ray images shown in Fig. 2).

Semi-quantitative assessment of defect fusion from 2 through 8 weeks using the radiographic scoring criteria described above revealed a progressive increase in mean defect mineralization each week, with 30 µg/mL rhBMP2 and higher achieving fusion by 6 weeks postoperation. These data are similar to previous results by others (Fig. 3).[19] However, there was no statistically significant difference observed in degree of mineralization between the 30, 150, 300, and 600 µg/mL rhBMP2-treated groups, with concentrations >30 µg/mL failing to promote defect mineralization faster.

microCT data

MicroCT analysis, three-dimensional reconstruction, and coronal sectional cuts revealed new bone formation in all groups. Lower concentrations of rhBMP2 at 5 and 10 µg/mL exhibited minimal new bone formation, with none of the samples achieving complete fusion (Fig. 3I, J). In contrast, at concentrations starting at 30 µg/mL and higher, a significant increase in bone volume was seen compared to lower doses, with complete fusion consistently achieved. Meanwhile, at concentrations of 150 µg/mL rhBMP and higher, the bone mass appeared significantly larger on surface microCT images (Fig. 3L–N), but did not demonstrate any statistically significant increase in bone volume (Fig. 4). In addition, poorer quality bone formation was observed at 150 µg/mL and above, with dose-dependent increases in cyst-like bone void formation in coronal cross-sectional cuts (Fig. 3S–U).

Femoral segmental defect histology

Histological evaluation of the femurs was consistent with radiographic findings, with the 0, 5, and 10 µg/mL rhBMP groups showing little evidence of bone formation (image not shown). A bone bridge was evident in all 30 µg/mL rhBMP2 samples (Fig. 5B, E, H, K). However, in the high-concentration groups (150, 300, and 600 µg/mL rhBMP2), H&E staining revealed a large bony structure that extended beyond the original defect (Fig. 5C, F, I, L; 150 and 300 µg/mL not shown). Longitudinal section through the 600 µg/mL specimen revealed little trabecular bone and, instead, an accumulation of adipocytes (Fig. 5C, F, I, L). Significantly, at the mid-range concentration of 30 µg/mL rhBMP2, the bone marrow space exhibited trabecular structure and cellularity that was more similar to normal bone marrow than the cyst-like bone voids observed in the 600 µg/mL rhBMP2 group. Masson's Trichrome staining, which identifies bone and osteoid matrix, confirmed the presence of mostly fibrous tissue in the rhBMP2-free control (Fig. 5J), trabecular bone resem-
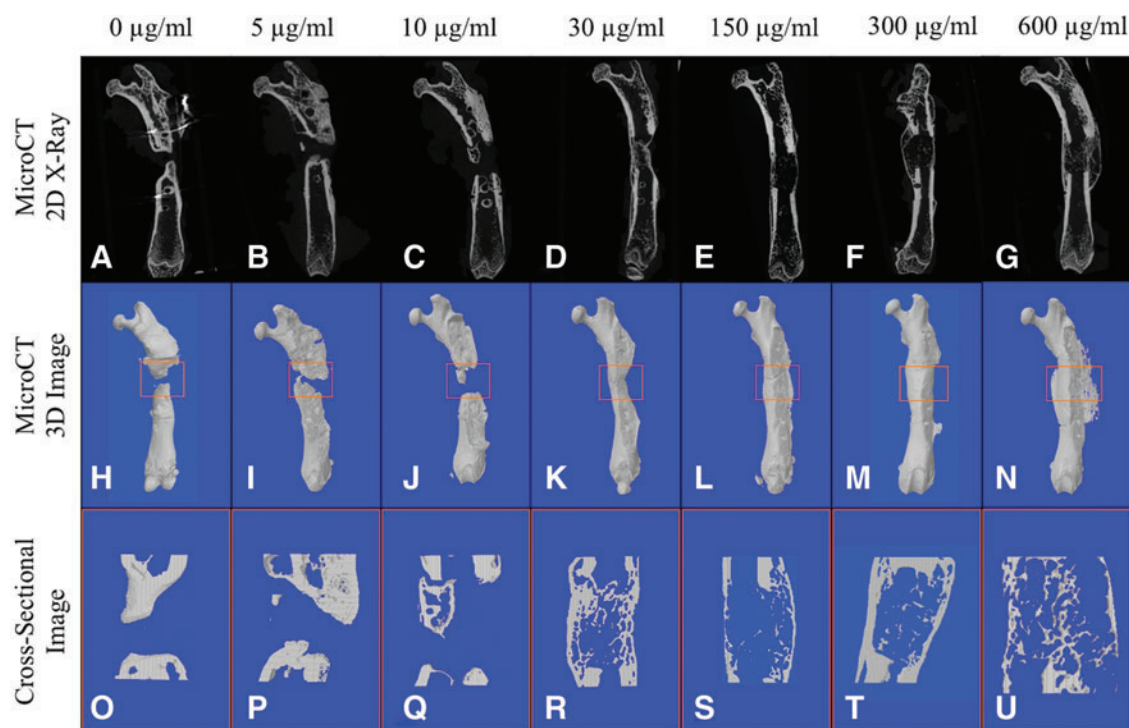
FIG. 2. Micro-computed tomography reconstruction of femoral segmental defect model. Representative two-dimensional reconstruction of femoral defects **(A–G)** and three-dimensional reconstruction **(H–N)** showing consistent fusion with concentrations of 30 μg/mL rhBMP2 and higher. Cyst-like bone formation was seen beginning at 150 μg/mL **(E, L)** and increase in size with higher concentrations of 300 and 600 μg/mL **(F, G, M, N)**. Coronal section cuts of these cyst-like structures revealed a thin bony shell that is hollow inside **(S–U)**, which was not observed at lower concentrations **(O–R)**. Color images available online at www.liebertonline.com/tea
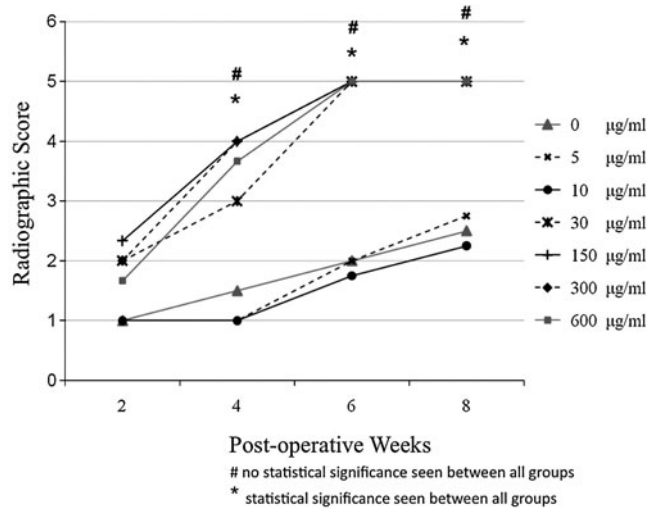
FIG. 3. Radiographic score of femoral segmental defect model. Semi-quantitative assessment of defect mineralization from week 2 through week 8. Kruskal–Wallis statistical analysis revealed a significant difference in mean defect mineralization between control and 5, 10, 30, 150, 300, and 600 μg/mL rhBMP2 at weeks 4, 6, and 8 ($^*p < 0.05$), but no statistically significant difference was seen when only 30 μg/mL rhBMP2 and higher concentrations of 150, 300, and 600 μg/mL rhBMP2 were compared at the same time points. rhBMP2, recombinant human bone morphogenetic protein.

bling normal bone at 30 μg/mL rhBMP2 (Fig. 5K), and adipocyte accumulation at 600 μg/mL rhBMP2 (Fig. 5L).

To further verify BMP-mediated bone formation and defect healing at 8 weeks, we performed immunohistochemistry staining for OCN, a matrix protein and marker for bone formation. More active bone formation was observed in the mid-range concentration of 30 μg/mL with strongest OCN staining (Fig. 5H), whereas higher concentrations of 150, 300, and 600 μg/mL rhBMP2 exhibited surprisingly less OCN staining and bone formation activity (Fig. 5I).

Onlay graft histology

Animals were sacrificed at 3, 7, and 14 days postimplantation. Palpation and gross observation did not reveal discernable swelling or surface inflammation after dissection of the hind limbs at all time points. Histological differences were observed between control and rhBMP2-containing sponges starting at 3 days postoperation, with increased inflammatory exudates present in rhBMP2-treated sponges (Fig. 6). By 7 days, a massive infiltration of large mono- and polymorphic nucleated cells was observed in the connective tissues within and surrounding the collagen sponges containing rhBMP2, but not in control sponges. This inflammatory response progressed in intensity up to 14 days, with appearance of osteoclast-like, multinucleated giant cells that stain positively with CTR, a G protein-coupled receptor that is a marker for osteoclastic differentiation (Fig. 7).[24,25]

FIG. 4. Comparison of new bone volume between treatment groups. Statistically significant difference in bone volume was found between all groups using analysis of variance. However, no statistically significant difference was found between mid to higher concentrations of 30, 150, 300, and 600 µg/mL rhBMP2-treated femurs, suggesting no increase in bone formation despite use of doses above 30 µg/mL. Color images available online at www.liebertonline.com/tea
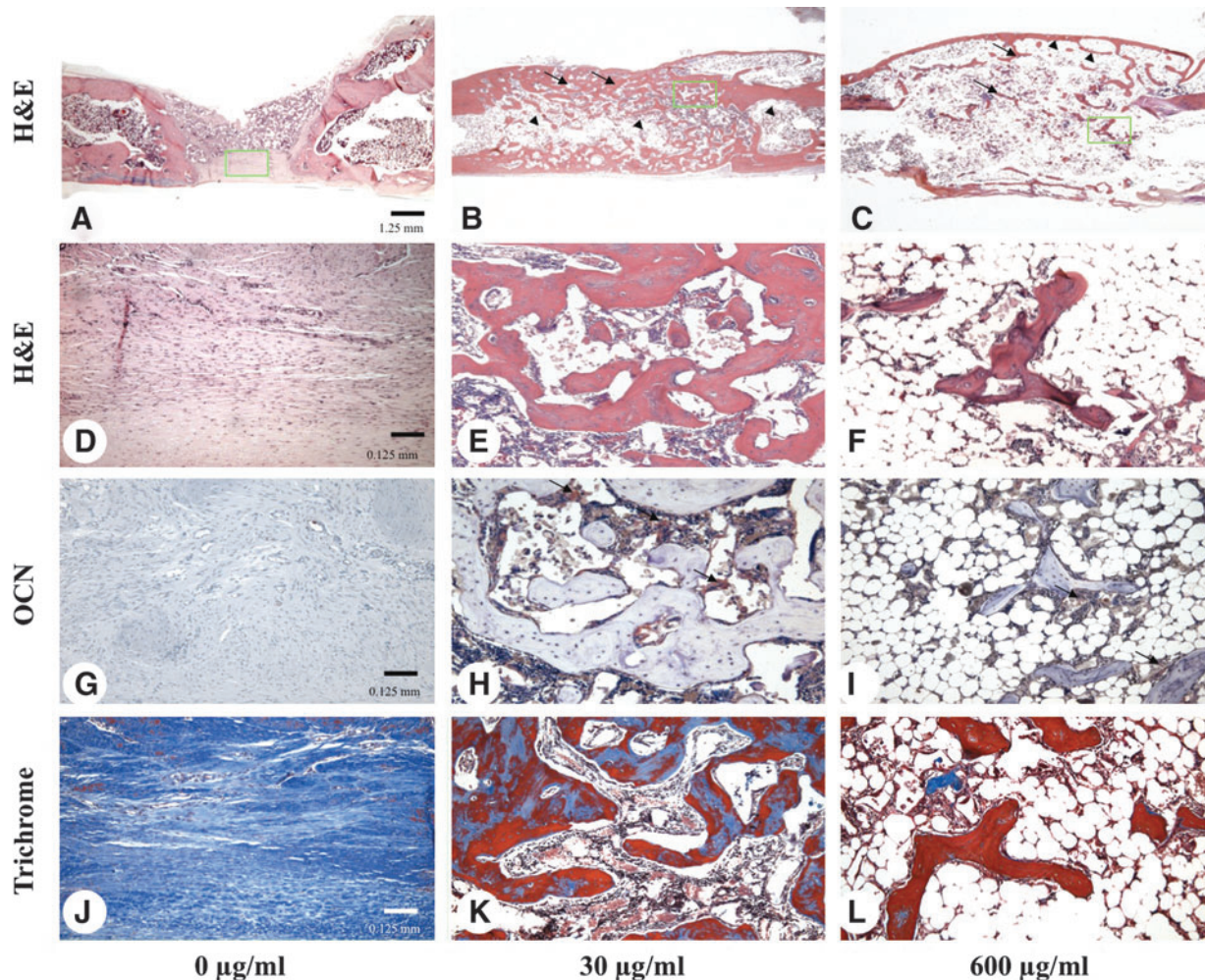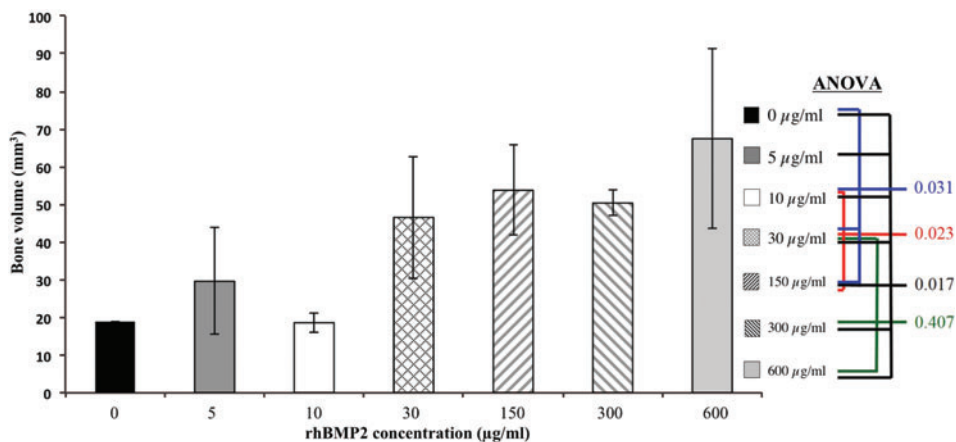
FIG. 5. Histological evidence of bone and cyst formation 8 weeks postoperation in femoral segmental defect model. **(A)** Low- and **(D)** high-power views of hematoxylin and eosin (H&E) histology show fibrotic defect union in the PBS-treated control group. Minimal new bone formation seen at both ends of the defect. The defect is filled with fibrotic tissue (arrow) rather than bridging bone. **(B)** Low- and **(E)** high-power view H&E show complete bony fusion of the defect in animals treated with 30 µg/mL rhBMP. The trabecular bone (arrows) and surrounding marrow (arrowheads) dominantly occupy the defect area with signs of more mature bone remodeling. **(C)** Low- and **(F)** high-power view H&E show formation of a bony cyst-like void in the original defect area in animals treated with 600 µg/mL rhBMP2. The bone bridging the defect is thin-walled and resembles a bony cyst with scant trabecular bone (arrows) and abundant fatty marrow (arrowheads) filling the hollow space. **(G–I)** Immunohistochemical staining of OCN shows active bone formation. **(G)** No obvious OCN staining was seen in the control group, whereas samples from the mid-range group **(**30 µg/mL rhBMP2-treated sample shown in **H)** demonstrate a strong positive brown staining of OCN (arrows). Less OCN expression **(I)** was observed in the high-concentration (600 µg/mL rhBMP2) treated group. **(J–L)** Masson's Trichrome staining distinguishes mineralized tissue (red) from connective tissue (blue). **(J)** The control group exhibited mostly fibrous connective tissue, whereas the 30 µg/mL rhBMP2 group **(K)** contained mature and actively remodeling bone and the 600 µg/mL rhBMP2 group **(L)** contained little trabecular bone but abundant adipose tissue. PBS, phosphate-buffered saline; OCN, osteocalcin.
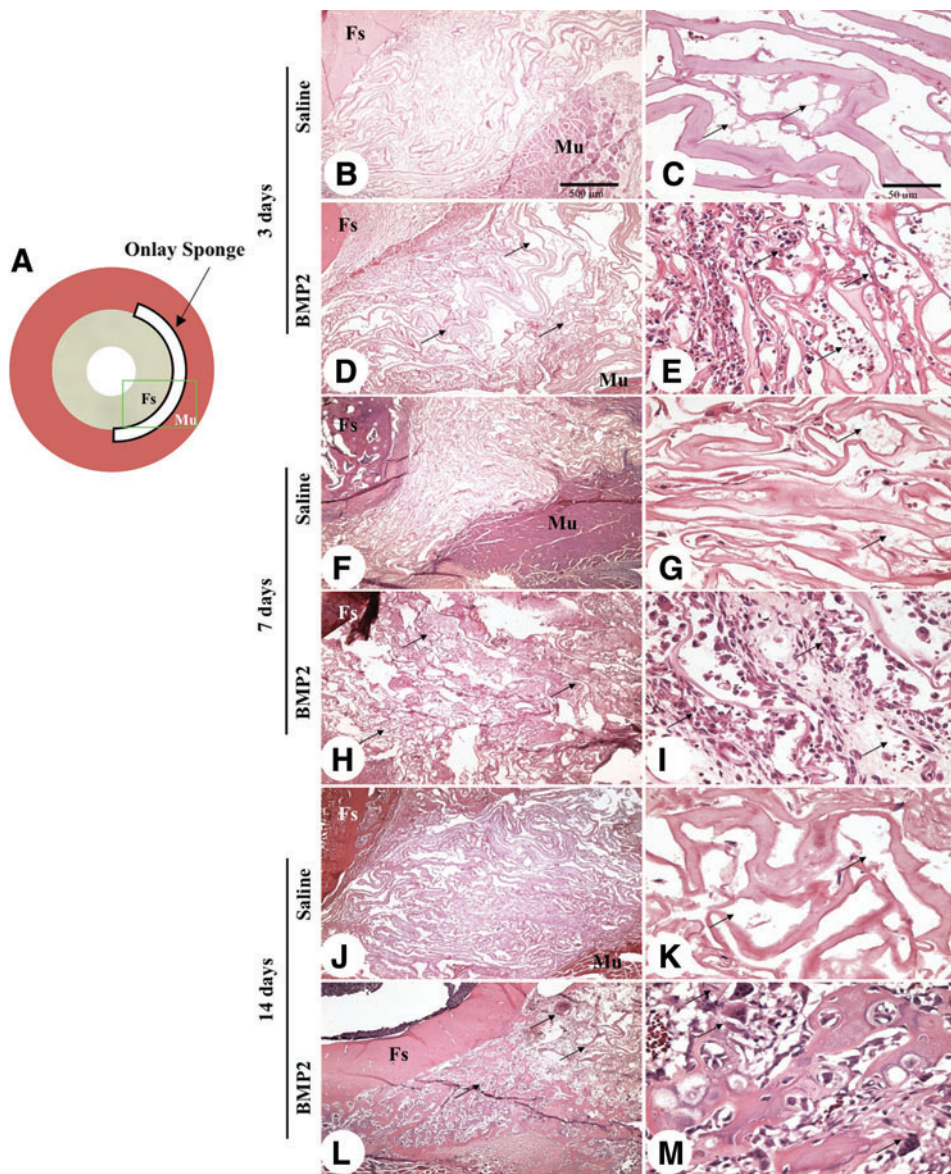
FIG. 6. Histology of BMP2 onlay model. **(A)** Schematic of femoral onlay model, with green rectangle depicting the orientation of the histological images. **(B)** Tissue profile of onlay experiment illustrating the position of collagen sponge scaffold on the surface of femoral shaft (Fs) with coverage by thigh muscles (Mu). **(C)** Representative high-power view of collagen sponge loaded with PBS in **(B)** appears normal with very minimal exudate (arrows) or cellularity at 3 days postoperation. **(D)** Low- and **(E)** high-power views of the onlay with BMP2-loaded collagen sponges. There is a significant number of inflammatory cells infiltrating between the fibers of collagen sponge (arrows) at this early time point as well as a more prominent exudative response. **(F)** Low- and **(G)** high-power views of the onlay with PBS control collagen sponges showing few exudates (arrows) and minimal cellular infiltrates at 7 days postoperation. **(H)** Low- and **(I)** high-power views of the onlay with BMP2-loaded collagen sponges at 7 days postoperation. There is profoundly increased inflammatory infiltration and exudates within the onlay area, which also extends significantly into the adjacent soft tissues. The cellular and fibrinous acellular exudates are prominently interspersed between the fibers of collagen sponge and were the dominating feature of the entire onlay region (arrows in **H**). Closer view of the peripheral area of the onlay region demonstrates some inflamed granulation tissues (arrows in **I**) at 7 days postoperation. **(J)** and **(K)** are images of the onlay with PBS control collagen sponges at 14 days postoperation showing minimal change in the normal collagen sponge fiber pattern from 7 days postoperation (arrows). **(L)** Low- and **(M)** high-power views of the onlay tissue with BMP2-loaded collagen sponges at 14 days postoperation. In addition to the dominant component of inflammatory infiltration (arrows in **L**) seen in **(H)** in the onlay area, many osteoclast-like multinuclear cells are also seen along the newly formed bone trabeculae (arrow in **M**). Fs, femoral shaft; Mu, thigh muscles. Scale bars: 500 μm for **B, D, F, H, J,** and **L** and 50 μm for **C, E, G, I, K,** and **M**. Color images available online at www.liebertonline.com/tea

Discussion

Using rodent models, we successfully and consistently reproduced two adverse effects of high-dose BMP2 *in vivo*: formation of cyst-like bone voids and inflammatory soft tissue swelling. With respect to bone formation in the femoral segmental defect model, we established three BMP2 concentration ranges, in a 75 μg volume, with the following outcomes: (1) sub-therapeutic concentrations with bony nonunion (0, 5, and 10 μg/mL); (2) therapeutic concentration with robust bony union, normal trabecular architecture, and marrow cellularity (30 μg/mL); and (3) supra-therapeutic concentrations with bony union accompanied by cyst-like bone devoid of normal bone structure and cellularity (150, 300, and 600 μg/mL). These findings indicate that increasing BMP2 beyond a certain threshold concentration does not improve bone healing, and may actually promote lower quality bone with abnormal structure and potentially inferior mechanical properties.

The resulting disparate phenotypes from our study, obtained by merely altering BMP2 concentration, reflect known pleiotropic effects of BMP2.[4,5,26,27] At doses required for human bone formation, and consistently demonstrated here when high-dose BMP2 was applied, BMP2 induced

FIG. 7. Significantly increased CTR-positive staining cells in the BMP2 onlay model. **(A)** Low- and **(B)** high-power images showing CTR-positive cells (arrows) scattered between fibers of the PBS-loaded collagen sponge at 3 days postoperation. **(C)** Low- and **(D)** high-power images showing significantly more CTR-positive cells (arrows) infiltrating the BMP2-loaded collagen sponges at 3 days postoperation. Most of the positive cells were large with rich cytoplasm with multinuclear cells also present (arrowheads). **(E)** Low- and **(F)** high-power views of CTR staining in the PBS onlay collagen sponge at 7 days postoperation show few positive cells with very faint staining (arrows in **F**). In contrast, the images of **(G)** and **(H)** from the BMP2 onlay collagen sponge at 7 days postoperation show significantly more CTR-positive cells (arrows), but much less than at 3 days postoperation in BMP2 treated collagen sponges **(D)**. Scale bars: 100 µm for **A, C, E,** and **G** and 50 µm for **B, D, F,** and **H**. CTR, calcitonin receptor.
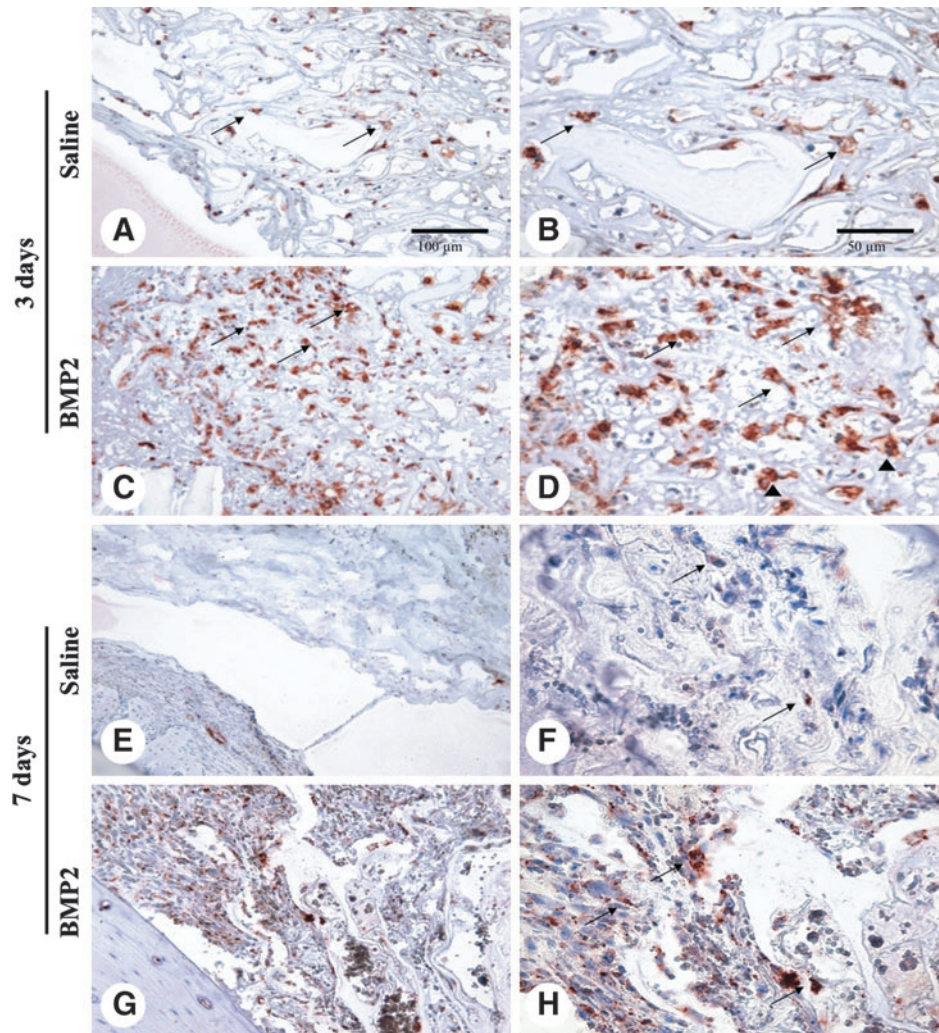
formation of cyst-like bone voids filled with fatty marrow instead of normal trabecular bone structure despite complete bone union. These results recapitulate those found by another group who demonstrated formation of bone voids in canine radii treated with high doses of BMP2.[28] In our study, we also specifically confirmed that the bone voids in our model contained adipose tissue. The presence of adipose tissue can be explained on a molecular level, based on published reports by others[29,30] that BMP2 can induce adipogenesis in addition to, or instead of, osteogenesis through activation of the transcription factor peroxisome proliferator-activated receptor gamma (PPARγ), a key regulator of adipocyte commitment.[31,32] Published studies have shown that PPARγ activation leads bone marrow stem cells to differentiate into adipocytes rather than osteoblasts,[32–34] as adipogenic programs in marrow are activated and osteogenic programs are suppressed.[35] Our histological results support this, as marrow cavities of femurs treated with high concentrations of BMP2 were predominantly filled with adipocytes. The increased adipogenesis mediated by high concentrations of BMP2 likely occurs not only through direct PPARγ activation, but through repression of the Wnt signaling pathway, which is known to downregulate adipogenesis.[32] We have validated this through *in vivo* experiments in which we successfully suppressed the for-

mation of cystic bone voids from high-dose BMP2 through co-application of Wnt signaling pathway activators (unpublished data, and [30]). Overall, the high concentrations of BMP2 required for human osteogenesis can dysregulate Wnt signaling and activate PPARγ to promote adipogenesis over osteoblastogenesis,[36] leading to inconsistent bone formation as well as decreased bone quality as demonstrated by our results.

Clinically, many exaggerated inflammatory reactions related to BMP2 use have been increasingly reported, including dysphagia and difficulty breathing in cervical spine fusion,[37] radiculopathies in lumbar spine fusion,[38] and limb edema in the treatment of unicameral bone cysts.[39] On CT imaging, these adverse effects have been attributed to presence of soft tissue inflammation and swelling at the surgical site,[40] but the molecular basis of these reactions has been largely unknown. To begin addressing the cellular and molecular basis for BMP2-mediated soft tissue swelling and inflammation, we employed a minimally traumatic femoral onlay model dosed with 4 mg/mL BMP2. This model was designed to assess short-term BMP-induced inflammation, which has been most commonly reported beginning on postoperative day 3 in one clinical study.[6] Another report demonstrated that BMP2-associated swelling peaks at 1 week after implantation in the cervical spine, and begins to

resolve 1 week thereafter.[7] Thus, to follow this trajectory, we selected 3, 7, and 14 days postimplantation for our experimental timepoints, and specifically emphasized the 7-day timepoint because it reflected the peak of the inflammation. At each timepoint, we performed a control where both legs were implanted with control Helistat sponges containing only PBS, to rule out systemic effects of collagen sponge implantation unrelated to BMP-induced inflammation,[40,41] which would confound our results. In addition, we also performed intra-animal controls in which a rat implanted with a BMP-impregnated sponge in one leg was implanted with a PBS control sponge in the other leg, to rule out BMP-induced inflammation in one limb influencing the contralateral limb.[42] As a result of these additional controls, we have an increased number of control onlays compared to BMP-impregnated onlays.

Our onlay model was able to consistently induce these inflammatory reactions, and sheds insight into the mechanism by which this reaction to BMP2 occurs. We demonstrate for the first time the cellular components of these soft tissue swellings with histological results of our onlay model showing a reproducible phenotype of significantly increased inflammatory infiltrates, including mono- and poly-morphonuclear cells and CTR-positive osteoclast-like cells, in BMP2-treated femurs compared to controls at 3, 7, and 14 days. The time course of the inflammatory response in our experiments agrees with, and may mechanistically explain, published clinical reports of excessive swelling with BMP2 use in anterior cervical discectomy, as swelling complications occur on postoperative day 4 on average (range 1 to 7 days) and last up to 21 days.[6,7,43,44]

BMP2 participates in a number of molecular pathways that may contribute both to our experimental results and effects reported in the clinical literature. The inflammatory response is not unexpected, as BMP2 is a known chemoattractant for lymphocytes, monocytes, and macrophages.[45] Moreover, BMP2 can also induce osteoclastogenesis by potentiating receptor activator of nuclear factor-kB ligand, a cytokine essential for inducing osteoclast differentiation.[46–48] Repression of Wnt signaling by high-dose BMP2 decreases osteoblast expression of osteoprotegerin, a member of the tumor necrosis factor receptor family that inhibits receptor activator of nuclear factor-kB ligand.[49–51] Additionally, up-regulation of PPARγ by BMP2, either directly or as a result of Wnt repression (which is known to downregulate PPARγ), would also increase osteoclasts, since PPARγ upregulates c-fos expression, an essential mediator of osteoclastogenesis.[52] Thus, high-dose BMP2 not only induces significant tissue inflammation that explains the clinically observed cervical swelling, but also increases osteoclastogenesis that may manifest clinically as vertebral subsidence or collapse and excessive bone resorption.[7,53,54]

Conclusion

BMP2 is a potent osteoinductive molecule with undesirable and reproducible dose-dependent side effects that include cyst-like bone void formation that can diminish the quality of regenerated bone and inflammation that can have life-threatening results. To improve patient safety and efficacy, there is an urgent need for strategies to suppress non-osteogenic BMP2 signaling targets by combining it with other growth factors to dampen unwanted inflammatory and adipogenic induction, or by decreasing BMP2 dose requirements through better control of BMP2 release and retention at the implantation site.

Disclosure Statement

Bone Biologics, Inc., licensed Nell-1-related patents from UCLA. C.S., K.T., B.M.W., and X.Z. are founders of Bone Biologics, Inc., and inventors on related patents.

References

1. Carlisle, E., and Fischgrund, J.S. Bone morphogenetic proteins for spinal fusion. Spine J **5,** 240S, 2005.
2. McKay, B., and Sandhu, H.S. Use of recombinant human bone morphogenetic protein-2 in spinal fusion applications. Spine **27,** S66, 2002.
3. Walker, D.H., and Wright, N.M. Bone morphogenetic proteins and spinal fusion. Neurosurg Focus **13,** 1, 2002.
4. Wong, D.A., Kumar, A., Jatana, S., Ghiselli, G., and Wong, K. Neurologic impairment from ectopic bone in the lumbar canal: a potential complication of off-label PLIF/TLIF use of bone morphogenetic protein-2 (BMP-2). Spine J **8,** 1011, 2008.
5. Kaneko, H., Arakawa, T., Mano, H., Kaneda, T., Ogasawara, A., Nakagawa, M., *et al.* Direct stimulation of osteoclastic bone resorption by bone morphogenetic protein (BMP)-2 and expression of BMP receptors in mature osteoclasts. Bone **27,** 479, 2000.
6. Smucker, J.D., Rhee, J.M., Singh, K., Yoon, S.T., and Heller, J.G. Increased swelling complications associated with off-label usage of rhBMP-2 in the anterior cervical spine. Spine **31,** 2813, 2006.
7. Vaidya, R., Carp, J., Sethi, A., Bartol, S., Craig, J., and Les, C.M. Complications of anterior cervical discectomy and fusion using recombinant human bone morphogenetic protein-2. Eur Spine J **16,** 1257, 2007.
8. Bagaria, A., and Prasada, V. Bone morphogenetic protein: current state of filed and the road ahead. J Orthop **2,** e3, 2005.
9. Boden, S.D., Kang, J., Sandhu, H., and Heller, J.G. Use of recombinant human bone morphogenetic protein-2 to achieve posterolateral lumbar spine fusion in humans: a prospective, randomized clinical pilot trial: 2002 Volvo Award in clinical studies. Spine (Phila Pa 1976) **27,** 2662, 2002.
10. McKay, W. Science-based assessment: accelerating product development of combination medical devices. Presented at the NMAB Roundtable on Biomedical Engineering Materials and Applications, Washington, DC, 2004.
11. FDA. InFUSE Bone Graft/LT-CAGE Lumbar Tapered Fusion Device. Summary of Safety and Effective Data Premarket Approval Application P000058, Rockville, MD, 2002.

12. Einhorn, T.A., Lane, J.M., Burstein, A.H., Kopman, C.R., and Vigorita, V.J. The healing of segmental bone defects induced by demineralized bone matrix. A radiographic and biomechanical study. J Bone Joint Surg Am 66, 274, 1984.

13. Alberius, P., and Gordh, M. Failure of onlay bone grafts to integrate over the calvarial suture: observations in adult isogeneic rats. J Craniomaxillofac Surg 24, 251, 1996.

14. Chou, Y.F., Dunn, J.C., and Wu, B.M. In vitro response of MC3T3-E1 pre-osteoblasts within three-dimensional apatite-coated PLGA scaffolds. J Biomed Mater Res B Appl Biomater 75, 81, 2005.

15. Lee, M., Li, W., Siu, R.K., Whang, J., Zhang, X., Soo, C., et al. Biomimetic apatite-coated alginate/chitosan microparticles as osteogenic protein carriers. Biomaterials 30, 6094, 2009.

16. Isobe, M., Yamazaki, Y., Mori, M., and Amagasa, T. Bone regeneration produced in rat femur defects by polymer capsules containing recombinant human bone morphogenetic protein-2. J Oral Maxillofac Surg 57, 695, 1999; discussion 9.

17. Lee, S.C., Shea, M., Battle, M.A., Kozitza, K., Ron, E., Turek, T., et al. Healing of large segmental defects in rat femurs is aided by RhBMP-2 in PLGA matrix. J Biomed Mater Res 28, 1149, 1994.

18. Zheng, Z., Yin, W., Zara, J.N., Li, W., Kwak, J., Mamidi, R., et al. The use of BMP-2 coupled—nanosilver-PLGA composite grafts to induce bone repair in grossly infected segmental defects. Biomaterials 31, 9293, 2010.

19. Yasko, A.W., Lane, J.M., Fellinger, E.J., Rosen, V., Wozney, J.M., and Wang, E.A. The healing of segmental bone defects, induced by recombinant human bone morphogenetic protein (rhBMP-2). A radiographic, histological, and biomechanical study in rats. J Bone Joint Surg 74, 659, 1992.

20. Lieberman, J.R., Daluiski, A., Stevenson, S., Wu, L., McAllister, P., Lee, Y.P., et al. The effect of regional gene therapy with bone morphogenetic protein-2-producing bone-marrow cells on the repair of segmental femoral defects in rats. J Bone Joint Surg Am 81, 905, 1999.

21. Wu, G., Liu, Y., Iizuka, T., and Hunziker, E.B. Biomimetic coating of organic polymers with a protein-functionalized layer of calcium phosphate: the surface properties of the carrier influence neither the coating characteristics nor the incorporation mechanism or release kinetics of the protein. Tissue Eng Part C Methods 16, 1255, 2010.

22. Immunologic response to collagen-impregnated vascular grafts: a randomized prospective study. The Canadian Multicenter Hemashield Study Group. J Vasc Surg 12, 741, 1990.

23. Kirker-Head, C., Karageorgiou, V., Hofmann, S., Fajardo, R., Betz, O., Merkle, H.P., et al. BMP-silk composite matrices heal critically sized femoral defects. Bone 41, 247, 2007.

24. Quinn, J.M., Morfis, M., Lam, M.H., Elliott, J., Kartsogiannis, V., Williams, E.D., et al. Calcitonin receptor antibodies in the identification of osteoclasts. Bone 25, 1, 1999.

25. Takahashi, S., Goldring, S., Katz, M., Hilsenbeck, S., Williams, R., and Roodman, G.D. Downregulation of calcitonin receptor mRNA expression by calcitonin during human osteoclast-like cell differentiation. J Clin Invest 95, 167, 1995.

26. Smucker, J.D., Rhee, J.M., Singh, K., Yoon, S.T., and Heller, J.G. Increased swelling complications associated with off-label usage of rhBMP-2 in the anterior cervical spine. Spine (Phila Pa 1976) 31, 2813, 2006.

27. Dmitriev, A.E., Farhang, S., Lehman, R.A., Jr., Ling, G.S., and Symes, A.J. Bone morphogenetic protein-2 used in spinal fusion with spinal cord injury penetrates intrathecally and elicits a functional signaling cascade. Spine J 10, 16, 2010.

28. Sciadini, M.F., and Johnson, K.D. Evaluation of recombinant human bone morphogenetic protein-2 as a bone-graft substitute in a canine segmental defect model. J Orthop Res 18, 289, 2000.

29. Jin, W., Takagi, T., Kanesashi, S.N., Kurahashi, T., Nomura, T., Harada, J., et al. Schnurri-2 controls BMP-dependent adipogenesis via interaction with Smad proteins. Dev Cell 10, 461, 2006.

30. Aghaloo, T., Jiang, X., Soo, C., Zhang, Z., Zhang, X., Hu, J., et al. A study of the role of Nell-1 gene modified goat bone marrow stromal cells in promoting new bone formation. Mol Ther 15, 1872, 2007.

31. Rosen, E.D., and Spiegelman, B.M. PPARgamma: a nuclear regulator of metabolism, differentiation, and cell growth. J Biol Chem 276, 37731, 2001.

32. Takada, I., Kouzmenko, A.P., and Kato, S. Wnt and PPAR-gamma signaling in osteoblastogenesis and adipogenesis. Nat Rev Rheumatol 5, 442, 2009.

33. Takada, I., and Kato, S. Molecular mechanism of switching adipocyte/osteoblast differentiation through regulation of PPAR-gamma function. Clin Calcium 18, 656, 2008.

34. Justesen, J., Stenderup, K., Eriksen, E.F., and Kassem, M. Maintenance of osteoblastic and adipocytic differentiation potential with age and osteoporosis in human marrow stromal cell cultures. Calcif Tissue Int 71, 36, 2002.

35. Moerman, E.J., Teng, K., Lipschitz, D.A., and Lecka-Czernik, B. Aging activates adipogenic and suppresses osteogenic programs in mesenchymal marrow stroma/stem cells: the role of PPAR-gamma2 transcription factor and TGF-beta/BMP signaling pathways. Aging Cell 3, 379, 2004.

36. Krause, U., Harris, S., Green, A., Ylostalo, J., Zeitouni, S., Lee, N., et al. Pharmaceutical modulation of canonical Wnt signaling in multipotent stromal cells for improved osteoinductive therapy. Proc Natl Acad Sci USA 107, 4147, 2010.

37. Mroz, T.E., Wang, J.C., Hashimoto, R., and Norvell, D.C. Complications related to osteobiologics use in spine surgery: a systematic review. Spine (Phila Pa 1976) 35, S86, 2010.

38. Mindea, S.A., Shih, P., and Song, J.K. Recombinant human bone morphogenetic protein-2-induced radiculitis in elective minimally invasive transforaminal lumbar interbody fusions: a series review. Spine (Phila Pa 1976) 34, 1480, 2009; discussion 5.

39. MacDonald, K.M., Swanstrom, M.M., McCarthy, J.J., Nemeth, B.A., Guliani, T.A., and Noonan, K.J. Exaggerated inflammatory response after use of recombinant bone morphogenetic protein in recurrent unicameral bone cysts. J Pediatr Orthop 30, 199, 2010.

40. Mroz, T.E., Wang, J.C., Hashimoto, R., and Norvell, D.C. Complications related to osteobiologics use in spine surgery: a systematic review. Spine (Phila Pa 1976) 35, S86, 2010.

41. Kanayama, M., Hashimoto, T., Shigenobu, K., Yamane, S., Bauer, T.W., and Togawa, D. A prospective randomized study of posterolateral lumbar fusion using osteogenic protein-1 (OP-1) versus local autograft with ceramic bone substitute: emphasis of surgical exploration and histologic assessment. Spine (Phila Pa 1976) 31, 1067, 2006.

42. Shenker, N., Haigh, R., Roberts, E., Mapp, P., Harris, N., and Blake, D. A review of contralateral responses to a unilateral inflammatory lesion. Rheumatology (Oxford) 42, 1279, 2003.

43. Perri, B., Cooper, M., Lauryssen, C., and Anand, N. Adverse swelling associated with use of rh-BMP-2 in anterior cervical discectomy and fusion: a case study. Spine J 7, 235, 2007.

44. Buttermann, G.R. Prospective nonrandomized comparison of an allograft with bone morphogenic protein versus an iliac-crest autograft in anterior cervical discectomy and fusion. Spine J **8,** 426, 2008.

45. Cunningham, N.S., Paralkar, V., and Reddi, A.H. Osteogenin and recombinant bone morphogenetic protein 2B are chemotactic for human monocytes and stimulate transforming growth factor beta 1 mRNA expression. Proc Natl Acad Sci USA **89,** 11740, 1992.

46. Chan, B.Y., Gartland, A., Wilson, P.J., Buckley, K.A., Dillon, J.P., Fraser, W.D., *et al.* PPAR agonists modulate human osteoclast formation and activity *in vitro*. Bone **40,** 149, 2007.

47. Irie, K., Alpaslan, C., Takahashi, K., Kondo, Y., Izumi, N., Sakakura, Y., *et al.* Osteoclast differentiation in ectopic bone formation induced by recombinant human bone morphogenetic protein 2 (rhBMP-2). J Bone Miner Metab **21,** 363, 2003.

48. Itoh, K., Udagawa, N., Katagiri, T., Iemura, S., Ueno, N., Yasuda, H., *et al.* Bone morphogenetic protein 2 stimulates osteoclast differentiation and survival supported by receptor activator of nuclear factor-kappaB ligand. Endocrinology **142,** 3656, 2001.

49. Simonet, W.S., Lacey, D.L., Dunstan, C.R., Kelley, M., Chang, M.S., Luthy, R., *et al.* Osteoprotegerin: a novel secreted protein involved in the regulation of bone density. Cell **89,** 309, 1997.

50. Yasuda, H., Shima, N., Nakagawa, N., Yamaguchi, K., Kinosaki, M., Mochizuki, S., *et al.* Osteoclast differentiation factor is a ligand for osteoprotegerin/osteoclastogenesis-inhibitory factor and is identical to TRANCE/RANKL. Proc Natl Acad Sci USA **95,** 3597, 1998.

51. Glass, D.A., 2nd, Bialek, P., Ahn, J.D., Starbuck, M., Patel, M.S., Clevers, H., *et al.* Canonical Wnt signaling in differentiated osteoblasts controls osteoclast differentiation. Dev Cell **8,** 751, 2005.

52. Wan, Y., Chong, L.W., and Evans, R.M. PPAR-gamma regulates osteoclastogenesis in mice. Nat Med **13,** 1496, 2007.

53. Mannion, R.J., Nowitzke, A.M., and Wood, M.J. Promoting fusion in minimally invasive lumbar interbody stabilization with low-dose bone morphogenic protein-2-but what is the cost? Spine J 2010. doi:10.1016/j.spinee.2010.07.005

54. Vaidya, R., Weir, R., Sethi, A., Meisterling, S., Hakeos, W., and Wybo, C.D. Interbody fusion with allograft and rhBMP-2 leads to consistent fusion but early subsidence. J Bone Joint Surg Br **89,** 342, 2007.

Address correspondence to:
Chia Soo, M.D.
Department of Orthopaedic Surgery
School of Medicine
University of California, Los Angeles
675 Charles E. Young Dr. South
Room 2641A, MRL
Los Angeles, CA 90095-1759

E-mail: bsoo@ucla.edu